Physica B 407 (2012) 3457–3462

Contents lists available at SciVerse ScienceDirect

Physica B

journal homepage: www.elsevier.com/locate/physb

Spin glass behavior in hole- and electron-doped bismuth manganite single crystals

B.C. Zhao [a,*], Y.N. Huang [a], C.Y. Hao [b], G.L. Kuang [b], Y.P. Sun [a,b]

[a] Key Laboratory of Materials Physics, Institute of Solid State Physics, Chinese Academy of Sciences, Hefei 230031, People's Republic of China
[b] High Magnetic Field Laboratory, Chinese Academy of Sciences, Hefei 230031, People's Republic of China

ARTICLE INFO

Article history:
Received 14 February 2011
Received in revised form
18 April 2012
Accepted 1 May 2012
Available online 7 May 2012

Keywords:
Flux method
Charge ordering

ABSTRACT

The hole- and electron-doped bismuth manganites $Bi_{0.55}Ca_{0.45}MnO_3$, $Bi_{0.55}Sr_{0.45}MnO_3$ and $Bi_{0.95}Ce_{0.05}MnO_3$ single crystals were grown using the flux-growth method. Their structural, magnetic and electrical transport properties have been compared studied. All samples show spin-glass magnetic behavior at low temperatures. In the immediate temperature region, an antiferromagnetic transition at T_A and a charge-ordering state at T_{CO} are observed for $Bi_{0.55}Ca_{0.45}MnO_3$ crystal, whereas only an antiferromagnetic transition exists in $Bi_{0.95}Ce_{0.05}MnO_3$ and $Bi_{0.55}Sr_{0.45}MnO_3$ crystals. $Bi_{0.55}Ca_{0.45}MnO_3$ and $Bi_{0.55}Sr_{0.45}MnO_3$ samples show semiconducting transport behavior in the whole studied temperature range, whereas $Bi_{0.95}Ce_{0.05}MnO_3$ is an insulator at room temperature. In addition, near T_{CO} a positive magnetoresistance as large as 70.7% is observed for $Bi_{0.55}Ca_{0.45}MnO_3$ sample under 5 T applied magnetic field. The obtained results may originate from the rotation of the polarized Bi-$6s^2$ lone pair electrons in the magnetic field.

1. Introduction

Since the discovery of the colossal magnetoresistance (CMR) effect in perovskite manganites with general formula $R_{1-x}A_xMnO_3$ (where R is a trivalent cation and A a divalent or tetravalent cation), a great deal of attention has been focused on these compounds due to their unusual electronic states and physical properties [1–3]. The interest has both a fundamental and an applied perspective. In terms of the latter these system may have the possibility to fabricate sensor and storage devices based on CMR effect. The system also provide interesting possibilities for studying the complicated interplay between spin, charge, orbital, and lattice degrees in strong correlated systems.

Spin-glass behavior is a key issue in the studying of manganite systems, in which short-range ferromagnetic (FM) clusters are considered to be embedded in an antiferromagnetic (AFM) matrix. The hypothesis has already been proved by various methods [4,5]. The spin glass behavior at low temperatures in manganite materials can be understood in terms of the competition between the FM ordering in the clusters and the AFM interactions present in the matrix. Under applied magnetic field, these FM clusters grow up and eventually coalesce, leading to the completing of the apparent FM ordering [6]. Charge-ordering phenomenon is another key issue in manganites, which is generally characterized by the direct space ordering of Mn^{3+} and Mn^{4+} ions [7]. At high temperatures these ions are randomly distributed within the MnO_2 planes in the lattice and become ordered arrangement upon cooling through a certain temperature. This order is usually accompanied by orbital order (OO), an ordered occupation of the e_g orbitals of the Mn ions. The CO state is expected to become stable when the repulsive Coulomb interaction between the carriers dominates over the kinetic energy of the carriers. Beyond this simple ionic model, ordered Zener polarons (ZP) were suggested as a more realistic scenario for the CO state in manganites [8]. In the ZP model, each e_g electron is considered to be trapped in a Mn–O–Mn trio. The two Mn ions in the trio conserve an intermediate valence state and are ferromagnetically coupled due to the double-exchange interaction induced by the shared e_g electrons.

The family of bismuth-based manganites $Bi_{1-x}A_xMnO_3$ has recently got much interest because of the physics lying behind the unusually high temperature charge ordering phase and the discovery of intrinsic phase separation [9,10]. The properties of bismuth-based oxides depend on the behavior of the highly polarizable $6s^2$ lone pair electrons of Bi^{3+} ions. Bi^{3+} ions have been found to push T_{CO} up to 600 K in $Bi_{0.75}Sr_{0.25}MnO_3$. This is the highest T_{CO} reported yet in the manganites [11]. $Bi_{1-x}Ca_xMnO_3$ is insulating for $0.2<x<1.0$, with CO at or above room temperature for $0.4\leq x\leq 0.6$ [9,12]. Its CO temperature is $T_{CO}=325$ K for $x=0.5$, it peaks at 335 K for $x=0.6$, and drops to 210 K in the Mn^{4+} rich region for $x=0.82$ [13]. Except for the CO phenomenon, spin clusters and spin-glass behavior are also observed in the $Bi_{1-x}Ca_xMnO_3$ system with $x\sim 0.875$ [14].

* Corresponding author. Tel.: +86 551 559 1439; fax: +86 551 559 1434.
E-mail address: bchzhao@issp.ac.cn (B.C. Zhao).

0921-4526/$ - see front matter © 2012 Elsevier B.V. All rights reserved.
http://dx.doi.org/10.1016/j.physb.2012.05.001

In this work, hole- and electron-doped bismuth-based crystals $Bi_{0.55}Ca_{0.45}MnO_3$, $Bi_{0.55}Sr_{0.45}MnO_3$ and $Bi_{0.95}Ce_{0.05}MnO_3$ have been synthesized. Detailed structural, magnetic, and transport characterization have been performed on the obtained crystals. The results show that spin-glass behavior is a common feature for these samples.

2. Experimental procedure

Single crystals of $Bi_{0.55}Ca_{0.45}MnO_3$, $Bi_{0.55}Sr_{0.45}MnO_3$ and $Bi_{0.95}Ce_{0.05}MnO_3$ were grown by the flux melting technique using Bi_2O_3 as the flux. The precursors Bi_2O_3, $CaCO_3$, $SrCO_3$, CeO_2 and MnO_2 were weighed and mixed thoroughly in Bi:(Ce, Ca, Sr):Mn=0.7:0.3:1 ratio and pre-heated twice at 900 °C for 24 h. The obtained powder with 5 times molar Bi_2O_3 was ground, pressed and then put into a platinum crucible. The growth was performed in a muffle furnace. The furnace was first heated to 1050 °C and kept at this temperature for 10 h to ensure sufficient melting, mixing and reaction of the raw materials. It was then cooled to 830 °C at a rate of 1 °C/h and finally cooled rapidly down to room temperature at a rate of about 200 °C/h in order to avoid possible twinning. Black tetrahedral-like $Bi_{0.95}Ce_{0.05}MnO_3$ and rectangular-like $Bi_{0.55}(Ca,Sr)_{0.45}MnO_3$ single-crystals could be extracted from the exposed surface and cavities within the solidified flux. The typical size of the crystals is 0.5 mm and 3 mm × 2 mm × 1.5 mm for $Bi_{0.95}Ce_{0.05}MnO_3$ and $Bi_{0.55}(Ca, Sr)_{0.45}MnO_3$, respectively.

The structure and phase purity of the samples was checked by X-ray diffraction (XRD) using Cu K_α radiation at room temperature. The composition of the samples was determined by an energy dispersive spectroscopy (EDS) technique. The resistive measurements were performed with a Quantum Design physical properties measurement system (PPMS) using the Van der Pauw method. DC magnetization measurements were carried out with a vibrating sample magnetometer (VSM) attached to the PPMS system and ac susceptibility measurements were performed with a Quantum Design superconducting quantum interference device (SQUID) MPMS system.

3. Results and discussion

The nominal composition $Bi_{0.7}A_{0.3}MnO_3$ (A=Ca, Sr and Ce) and the growth process of the three samples studied in this work are the same. However, the obtained crystals are quite different in their actual composition, crystal shape and size. From the EDS analysis, the actual composition of Ca and Sr in the resulting crystals is about 0.45, whereas that of Ce is about 0.05. The difference may originate from the much smaller ionic size of Ce^{4+} ions compared to that of Sr^{2+}/Ca^{2+} (0.87, 1, and 1.18 for Ce^{4+}, Ca^{2+}, and Sr^{2+}, respectively) in a perovskite structure. Fig. 1(a) shows the room-temperature powder X-ray diffraction (XRD) patterns for the three studied materials. All the reflection peaks in the XRD pattern of $Bi_{0.55}Sr_{0.45}MnO_3$ can be indexed with the tetragonal perovskite structure, whereas the patterns of $Bi_{0.55}Ca_{0.45}MnO_3$ and $Bi_{0.95}Ce_{0.05}MnO_3$ can be indexed with the monoclinic and triclinic cell, respectively. The results are consistent with the earlier reported ones of similar compounds [15,16]. Moreover, θ–2θ X-ray diffraction was performed on one of the facets of the Ca- and Sr-doped crystals. As shown in Fig. 1(b), only sharp (1 0 0) family peaks are observed in the XRD patterns, indicating the single-crystal structure of the obtained samples.

We performed magnetic measurement with applied fields parallel (M_{ab}) and perpendicular (M_c) to the *ab* plane for both $Bi_{0.55}Sr_{0.45}MnO_3$ and $Bi_{0.55}Ca_{0.45}MnO_3$ samples. As shown in Fig. 2,

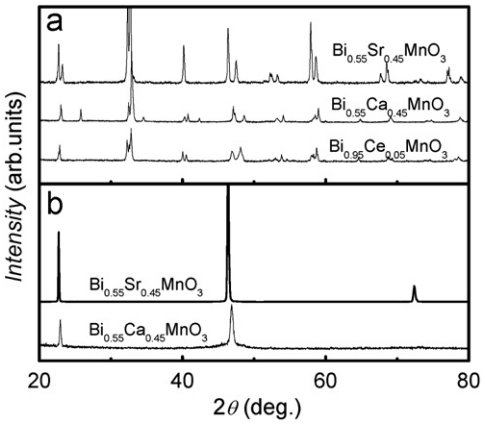

Fig. 1. (a) XRD patterns of powdered single crystals and (b) XRD patterns of the $Bi_{0.55}Ca_{0.45}MnO_3$ and $Bi_{0.55}Sr_{0.45}MnO_3$ single crystals.

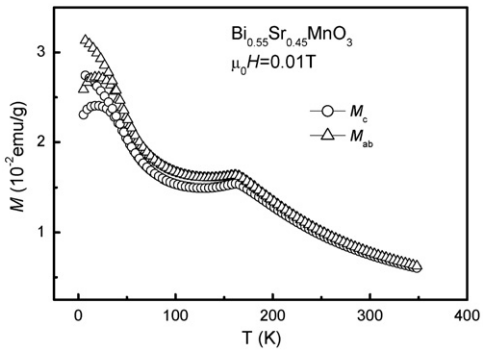

Fig. 2. DC magnetization as a function of temperature with applied magnetic field parallel (triangle) and perpendicular (circle) to the *ab* plane of the $Bi_{0.55}Sr_{0.45}MnO_3$ single crystal.

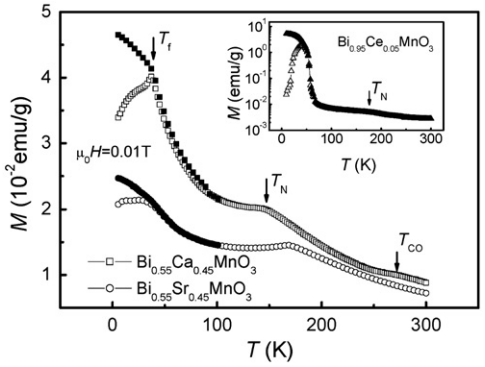

Fig. 3. The temperature dependence of DC magnetization for $Bi_{0.55}Ca_{0.45}MnO_3$ and $Bi_{0.55}Sr_{0.45}MnO_3$ samples in an applied magnetic field of 0.01 T. The inset shows the results for $Bi_{0.95}Ce_{0.05}MnO_3$ in a logarithmic scale.

the temperature dependence of M_{ab} and M_c of $Bi_{0.55}Sr_{0.45}MnO_3$ is almost the same, although M_{ab} is a little bit larger than M_c. In the following, all the magnetic measurements on $Bi_{0.55}Sr_{0.45}MnO_3$ and $Bi_{0.55}Ca_{0.45}MnO_3$ were performed with magnetic field parallel to the *ab* plane. Fig. 3 shows the temperature dependence of the DC magnetization $M(T)$ for the two samples. The $M(T)$ curve for $Bi_{0.95}Ce_{0.05}MnO_3$ is shown in its inset. The data are collected under both zero-field cooling (ZFC) and field cooling (FC) modes with an applied magnetic field of $\mu_0H=0.01$ T. A typical Hopkinson-type maximum exists at T_f in the ZFC curve and the low temperature ZFC and FC curves deviate substantially for all the samples. The phenomenon of the discrepancy between FC and ZFC magnetization